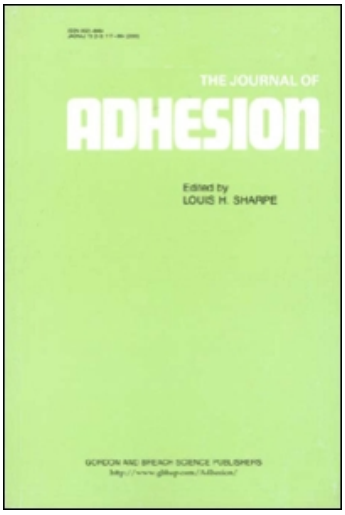

The Journal of Adhesion
Publication details, including instructions for authors and subscription information:
http://www.informaworld.com/smpp/title~content=t713453635

Interfacial Shear Strength of Oxide Films on Carbon Fibers Formed by the Sol-Gel Process

Taehwan Jung[ab]; R. V. Subramanian[a]
[a] Department of Mechanical and Materials Engineering, Washington State University, Pullman, WA, USA [b] JEIL Products Ltd., Korea

To cite this Article Jung, Taehwan and Subramanian, R. V.(1995) 'Interfacial Shear Strength of Oxide Films on Carbon Fibers Formed by the Sol-Gel Process', The Journal of Adhesion, 52: 1, 65 — 79
To link to this Article: DOI: 10.1080/00218469508015186
URL: http://dx.doi.org/10.1080/00218469508015186

J. Adhesion, 1995, Vol. 52, pp. 65–79
Reprints available directly from the publisher
Photocopying permitted by license only

Interfacial Shear Strength of Oxide Films on Carbon Fibers Formed by the Sol-Gel Process*

TAEHWAN JUNG[1] and R. V. SUBRAMANIAN[2]

Department of Mechanical and Materials Engineering, Washington State University, Pullman, WA 99164-2920, USA

(Received December 15, 1993; in final form May 4, 1994)

The bonding of oxide films on AU carbon fibers is investigated using the single-filament-composite (SFC) specimen. The oxide films were formed by first dip-coating fibers in solutions of zirconium-n-propoxide, zirconium-n-propoxide chelated by ethyl acetoacetate or a zircoaluminate inorganic polymer coordinated to methacryloxy and oleophilic ligands, followed by steam hydrolysis and thermal treatment. Coating uniformity and morphology were examined by SEM and EDXA.

Fiber strength distributions at different gage lengths were obtained from tensile strength measurements of single fibers, coated and uncoated, and analyzed by Weibull statistics. Fiber fragmentation in SFC specimens was also monitored to obtain the critical length, l_c. Fiber strength, σ_{sim}, at the critical length was predicted by numerical simulation using the bimodal distribution parameters experimentally determined. The simulation model of fragment distribution with respect to fiber strength in the SFC specimen was developed using Weibull statistics, and has been experimentally verified. The interfacial shear strength, τ, was calculated from σ_{sim} and l_c.

The predicted fiber strengths at the critical length, estimated by numerical simulation using bimodal distribution, agree with the extrapolated strengths using the experimental data; but overestimated strengths are obtained using the unimodal distribution model. The interfacial shear strength is increased slightly as the concentration of the coating solution increases to reach about 90% of the value for uncoated fibers with epoxy resin matrix. The level of bonding achieved between the fiber and coating is encouraging for potential use of the coated fiber in metal matrix composites.

KEY WORDS interfacial shear strength; carbon fiber strength; fiber coating by sol-gel process; zirconium oxide film; fiber strength at critical length; interface modification for metal matrix composites.

INTRODUCTION

Carbon fiber is preferred for reinforcement of metal matrix composites because the fiber combines light weight with high strength and modulus.[1] However, a serious limitation for using carbon fiber as a reinforcing material in metal matrix composites is the tendency for degradative chemical reactions to occur at the fiber-matrix interface. It

* Presented at the Seventeenth Annual Meeting of The Adhesion Society, Inc, in Orlando, Florida, U.S.A., February 21–23, 1994. One of a Collection of papers honoring Lawrence T. Drzal, the recipient in February 1994 of *The Adhesion Society Award for Excellence in Adhesion Science, Sponsored by 3M.*

[1] Present address: JEIL Products Ltd., Korea.

[2] Corresponding author.

is well known that the formation of a weak metal carbide interface has deleterious effects on the properties and performance of metal matrix composites. For example, the formation of aluminum carbide at the interface between the carbon fiber and aluminum matrix causes degradation of the fiber strength when the composite is used at high temperatures.[2]

In an effort to solve this problem, protective layers of glass or oxide are deposited on the carbon fiber surface.[3] The purpose of the oxide coating is to minimize degradative chemical reactions at the carbon fiber-metal matrix interface when the fiber is used as reinforcement in the fabrication and application of metal matrix composites. Thus, a thin film of silica was formed on the graphite fibers for application in a carbon fiber-reinforced magnesium composite system.[4] Also, in an earlier investigation from this laboratory, zirconia coating on graphite fiber was formed by thermal decomposition of $ZrOCl_2$ solution.[5] The choice of zirconia as a protective layer on carbon fiber was based on its thermal stability and chemical inertness.

In the present paper, zirconia and zircoaluminate coatings obtained by the sol-gel process are characterized. The effects of coatings on the carbon fiber strength, and the interfacial shear strength of the coatings are also evaluated.

EXPERIMENTAL

Coatings

The dip-coating method was used to deposit thin films of amorphous oxide on the carbon substrates. As substrates, Hercules high modulus untreated carbon fiber (AU-type fiber), pitch-based carbon monofilament (untreated, AVCO corp.) and graphite rod (untreated, National Electric Co.) were used. Coating solutions were prepared from zirconium-n-propoxide (Alpha Products Co.) and a zircoaluminate inorganic polymer coordinated to methacryloxy and oleophilic ligands (CAVCO Mod M-1, Cavedon Chemical Co., Inc.). Ethyl acetoacetate (Aldrich Chemical Co., Inc.) was used to stabilize the zirconium-n-propoxide and absolute ethanol was used as solvent.

Before the coating solutions were diluted by ethanol, the zirconium-n-propoxide (ZNP) was mixed with ethyl acetoacetate at a 1 to 1 molar ratio, and then stirred for 4 hours. The stabilized ZNP, and zircoaluminate complex (AZ) solutions were diluted with ethanol and stirred for 4 hours. The diluted solutions were stored in plastic containers. The AU fibers were affixed to stainless steel frames with aluminum tapes and dipped into the solutions for 2 minutes. The frames were withdrawn vertically at the speed of 20 cm/min. The coated fibers were exposed to hot steam (approximately 60°C) for 15 minutes to allow for hydrolysis to occur. These fibers were dried in air at room temperature for 6 hours and heat-treated at 180°C for 30 minutes.

The uniformity and morphology of the coatings on the fiber surface were examined by scanning electron microscopy (Hitachi S-570). The fibers were mounted onto aluminum studs and coated with gold using Hummer Technics V sputter coater in an argon atmosphere, for 6.5 minutes. Energy dispersive X-ray analysis (EDXA) was also used to identify the elements, Zr and Al existing on the surface of the coated fibers, using a Kevex 7000 unisystem installed on the SEM. The distribution of Zr and Al elements

through the coated surface was investigated by EDXA maps with Zr and Al signals. Prior to analysis, the samples were carbon coated using an Edwards evaporator.

The change of coating thickness as a function of concentration of the coating solutions was evaluated by the weight change after coating. In this experiment, the graphite rod (3 mm diameter) with 1 inch (25.4 mm) length was dipped into the solutions and withdrawn at the speed of 20 cm/min.

Fiber Strength

For measurement of tensile strength of fiber, a single fiber was aligned on a paper frame with rectangular hole of the same size as the gage length to be tested. The fiber was affixed to the frame with "5-minute" epoxy at the ends of the rectangular hole. Fiber diameter was measured using an American Optical I-60 microscope with a Vicker's image-splitting eyepiece attached. The frame was mounted onto a mini tensile testing machine built in-house and a cut was made on the sides of the rectangular hole, leaving the fiber connecting the two halves to carry the load. The fiber was finally strained at a crosshead speed of 1 mm/min and the fracture load was recorded on a chart by an $x-y$ recorder. The tensile strength distributions for each test were analyzed by the Weibull statistics.

SFC Test

The trends of interfacial properties between fiber and coatings under different conditions were determined by interfacial shear strength obtained from a single filament composite (SFC) test. In the case of the coated-fiber reinforced composite system, three failure mechanisms may occur; in one, failure can occur at the interface between coating surface and matrix; in another, failure can take place at the interface between fiber and coating, or in the third mechanism, failure may occur within the coating.

In our experiment, the failure is expected to take place between the coating and the carbon fiber rather than at the interface between the coating and the epoxy matrix since the carbon generally has a weak surface compared with the oxide. On the basis of this assumption, the interfacial shear strength between the coating and the carbon fiber can be evaluated. However, failure can take place inside the coating if the thickness of the coating is large, as, in fact, it was observed.

The SFC samples with a gage length of 22 mm and thickness about 1.8 mm were prepared by embedding a single fiber with a transparent epoxy resin in suitably designed silicone molds.[6] As a matrix, 10 grams of diglycidyl either of bisphenol-A (Epon 828; Shell Chemical Co.) was weighed out and diluted with 1 gram of phenyl glycidyl ether (Aldrich Chemical Co.). 1.45 grams of m-phenylenediamine (Aldrich Chemical Co.) was added to the mixture as a curing agent. This mixture was stirred at 65°C until the m-phenylenediamine was thoroughly dissolved in the epoxy resin. The fiber-embedded resin specimens were pre-heated at 80°C for 2 hours and cured at 150°C for 4 hours.

SFC specimens were tested by a hand-operated tensile loading device constructed in-house for straining the specimens. The SFC specimens were incrementally elongated, and the fiber breaks in the SFC specimen were observed using a Zeiss

fluorescence microscope with a polarized light attachment. At least five specimens were tested to obtain average fragment lengths. The successive breaks of the fiber were observed during elongation until no further fracture occurred, and the ultimate fragment lengths were measured. At this stage, sufficient stress to break the fiber is not transferred to the fiber because the fragment length is too short. The interfacial shear strength was calculated with experimentally obtained diameter, the critical length, and the fiber strength at the critical length predicted by a simulation model described in detail elsewhere,[7] and presented in outline below.

Simulation Model

In brief, as the fiber is broken successively during elongation of a SFC specimen, the relationships of the number of breaks (N) and the length of remaining fiber (L) with respect to the fiber strength(s), proposed by Curtin,[8]

$$\frac{dL}{ds} = -N\delta P(\delta;\eta)\frac{d\delta}{ds} \tag{1}$$

$$\frac{dN}{ds} = -NP(\delta;\eta)\frac{d\delta}{ds} + f(s, L^*) \tag{2}$$

$$L^* = N\int_{2\delta}^{\infty}(x-2\delta)P(x;\eta)dx \tag{3}$$

where δ is the recovery length which is equal to $l_c/2$, and η is δN/L. $P(\delta;\eta)$ is the unique strength fragment distribution;

$$P(\delta;\eta) = \frac{2}{\eta\delta}\int_0^{\eta}\psi(\eta')d\eta' \tag{4}$$

with

$$\psi(\eta) = \frac{\exp(-2\gamma)}{\eta^* - \eta} \tag{5}$$

where γ is Euler's constant ($=0.5772$) and η^* is 0.7476.

The strength distribution term in equation (2) based on the power series of Weibull distribution for the fiber length, L, is

$$f(s, L^*) = \frac{L^*}{L_o}\frac{m}{s_o}\left(\frac{s}{s_o}\right)^{m-1} \tag{6}$$

However, this strength distribution term would not be correct if the strength distribution in actual experiments shows multiple modes. Therefore, the strength distribution term needs to be modified to the multimodal term if necessary. Such a modified form of equation (6) for bimodal distribution is

$$f(s, L^*) = \frac{L^*}{L_o}\left\{P\frac{m_1}{s_{o1}}\left(\frac{s}{s_{o1}}\right)^{m_1-1} + q\frac{m_2}{s_{o2}}\left(\frac{s}{s_{o2}}\right)^{m_2-1}\right\} \tag{7}$$

where p and q are portions of low strength and high strength populations respectively, and m_1, m_2, s_{o1} and s_{o2} are the shape and scale factors for low and high strength portions, respectively.

The relationship between the fiber strength and fragmentation can be predicted by integrating the equations (1) and (2) with strength distribution terms from either equation (6) or (7). The differential equations can be solved easily using a numerical method with an iterative procedure. In this paper, the simulation is performed with Advanced Continuous Simulation Language (ACSL). From the simulation results, the fiber strength when there is a maximum number of breaks can be considered as the fiber strength at the critical length.

RESULTS AND DISCUSSION

The scanning electron micrograph (SEM) of carbon monofilaments (AVCO) coated by 5% ZNP solution is shown in Figure 1(a). The surface is smooth because of a thin and uniform coating. The uniform zirconia coating on the fiber surface was revealed by the energy dispersive X-ray map of the same fiber which was recorded using the zirconium signal (Fig. 1 (b)). The signal of Zr element is distributed through the whole surface of the fiber. Figure 2 shows (a) the SEM and (b) the energy dispersive X-ray map using the aluminum signal for the carbon monofilaments coated by the 5% AZ solution. The results are similar to Figure 1. From these results, it is found that thin and uniform coatings on the carbon fiber can be obtained from the ZNP solution as well as from the AZ solution.

Figure 3 shows scanning electron micrographs of AU fiber coated by ZNP solutions with various concentrations. For fiber coated from the 1% solution (Fig. 3(a)), a

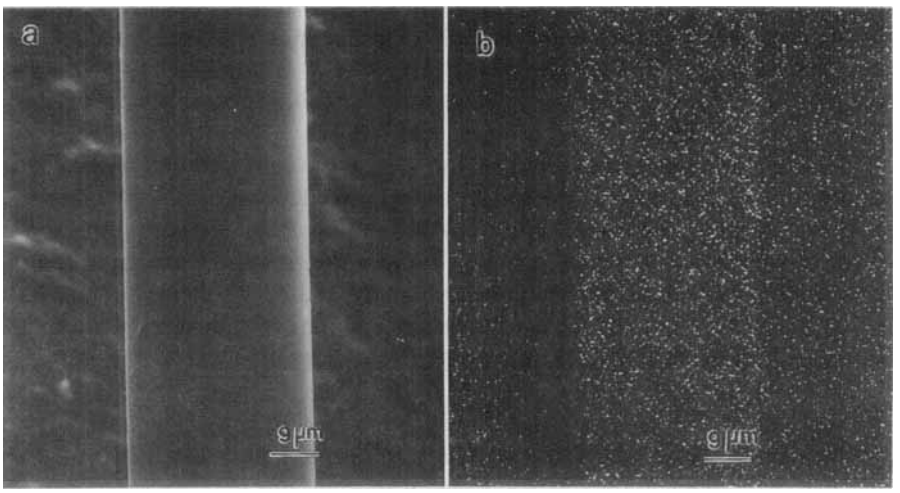

FIGURE 1 Scanning electron micrographs of (a) carbon monofilament coated by 5% ZNP solution and (b) its energy dispersive X-ray map recorded using the zirconium signal.

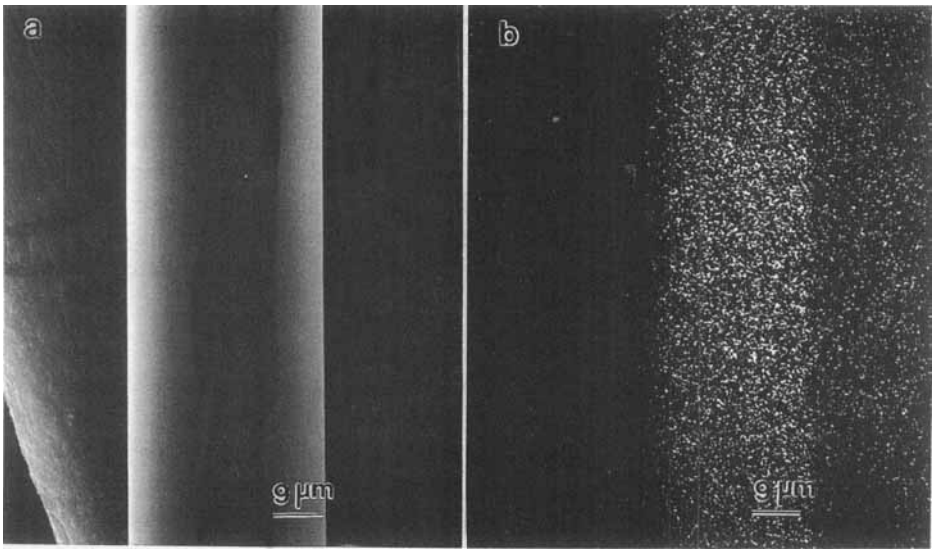

FIGURE 2 Scanning electron micrographs of (a) carbon monofilament coated by 5% AZ solution and (b) its energy dispersive X-ray map recorded using the aluminum signal.

uniformly-coated surface is observed. In the case of coating formed from a 5% solution, the surface coating is also uniform, in general (Fig. 3(b)), although occasionally the coated surface is pitted (Fig. 3(c)). However, non-uniformity in coating is frequently found at much higher concentrations of the coating solution, for example 20% in Figure 3(d). Such a non-uniformly coated surface, also observed with AZ solutions at higher concentrations, can be formed during evaporation of volatile species in the coating and cracking of the thick coating by shrinkage during hydrolysis and drying. The cracks in the coating on the fiber surface can initiate failure in the fiber and the composite matrix. The apparent interfacial shear strength would then be reduced since the cracks propagate through the coating. Therefore, it is important to arrive at an optimum thickness of the coating in order to ensure the desired performance of the coated fiber.

The change in coating thickness, as a function of the concentration of the coating solution, was estimated using the weight change per unit weight of a carbon rod as substrate. The increase in weight of the coating on the carbon rod with respect to the coating concentration is shown in Figure 4. From the figure, the weight of coatings increases with increasing concentration, for both AZ and ZNP solutions. A non-linear relation is observed between the weight change and the concentration of the coating solutions. From the data, the following experimental equation can be derived:

$$w = K \cdot c^n \tag{8}$$

where w is weight change which is dependent on thickness of the coating and c is the concentration of the coating solution, and K and n are constants obtained experimentally. The value of n was nearly 1.4 for both systems in this experiment. This nonlinearity comes from an increase in the viscosity of the solution with increasing concentration.[9] Also, it

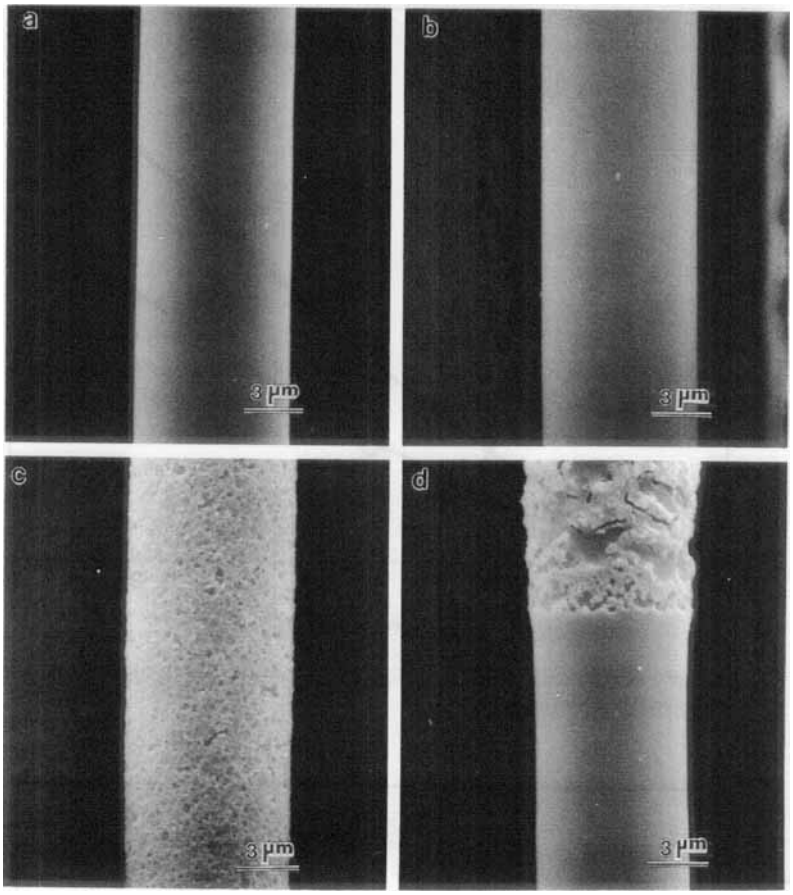

FIGURE 3 Scanning electron micrographs of AU fiber coated by ZNP solution with different concentration; a) 1%, b) 5%, c) 5%, d) 20%.

is to be noted that the coating obtained from the ZNP solution shows a larger weight increase than that from the AZ solution in the same concentration range.

Fiber Strength Distribution

The single fiber tensile test was used to investigate the fiber strength of the fibers coated under different conditions. The flaw distribution existing on the fiber was analyzed by Weibull statistics. Figure 5 shows estimated probability distributions of the tensile strengths for the AU fibers at different gage lengths.

The average strengths and Weibull parameters for the AU fibers at various gage lengths are presented in Table I. The strengths of the fiber at the tested gage lengths are distributed bimodally due to the presence of two kinds of defects. The low strength population, attributed to surface defects on the fiber, is decreased, and the high strength

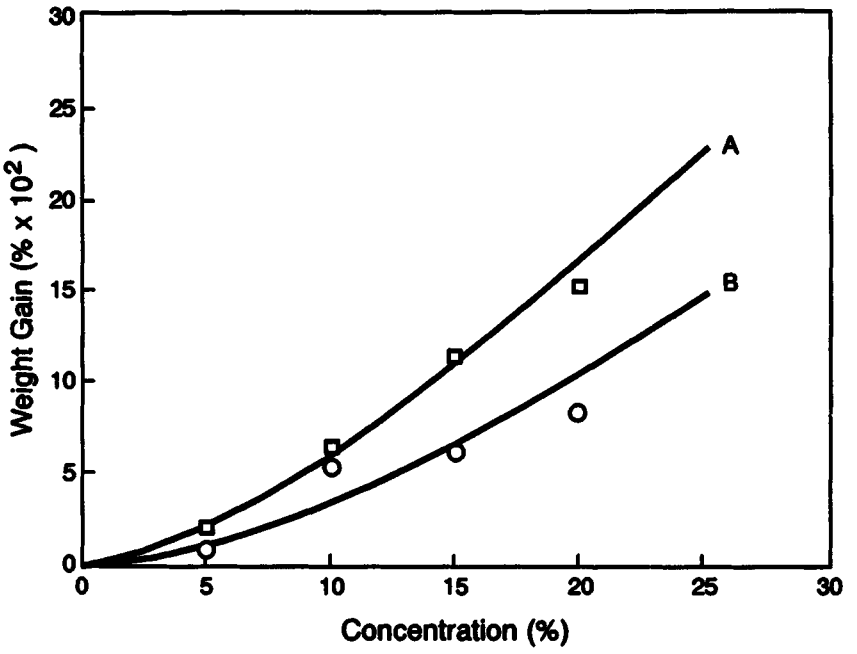

FIGURE 4 Effect of concentration of coating solutions on the change in net weight of coatings obtained from (a) AZ solution and (b) ZNP solution.

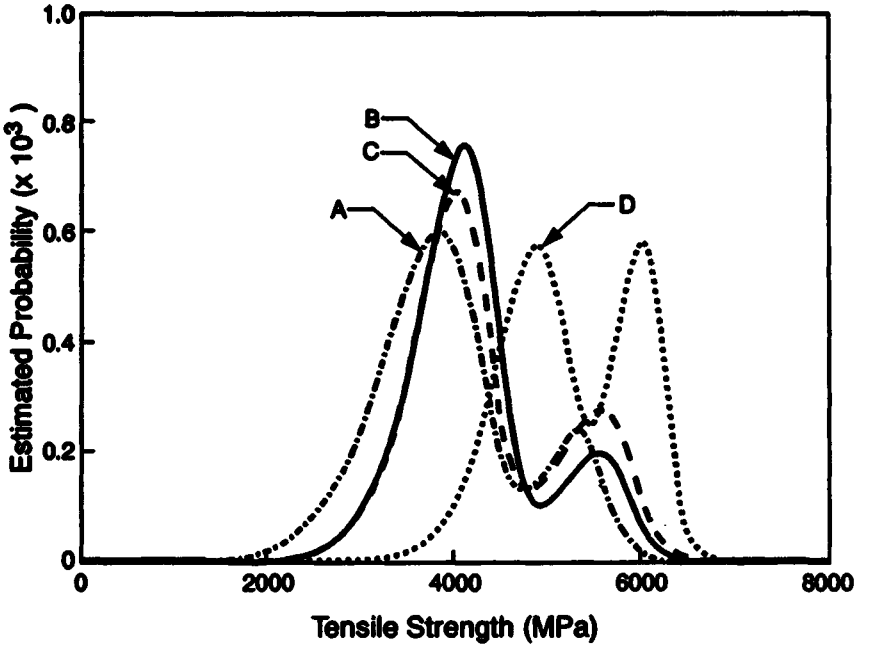

FIGURE 5 Bimodal Weibull distribution of untreated AU fibers at gage lengths: a) 22 mm, b) 10 mm, c) 6.5 mm, and d) 3 mm.

TABLE I
Average tensile strengths and parameters for Weibull distributions of AU-type carbon fibers with different gage lengths (L)

L(mm)	size	strength (MPa)	S.D.	p	Weibull m	s_o
22	39	4000	818	31/39	7.83	3914
				8/39	16.63	5398
					5.26*	4336(a)
10	39	4270	743	31/39	10.44	4160
				8/39	14.87	5619
					5.93*	4589(a)
6.5	37	4370	838	25/37	10.57	4079
				12/37	12.73	5604
					5.53*	4725(a)
3	32	5230	714	18/32	12.97	4894
				14/32	21.42	6055
					8.58*	5540(a)

p: ratios of low- and high-strength populations.
S. D.: standard deviation.
(*a*): Parameter for unimodal distribution.

population due to internal defects is increased, with decrease in the gage length. This is due to a reduced probability of the presence of surface damage in the fiber at the lower gage length. Interestingly, at the lowest gage length measured, 3 mm, the distribution is still bimodal, but the curve is changed significantly by the appearance of a new peak in the higher strength region. This reveals a different kind of defects, most probably internal defects, controlling the strength distribution at this gage length. The effect of the surface defects at the low end of the distribution curve is not significant at such short gage lengths, and the corresponding low strength population is absent.

Figure 6 and 7 show the Weibull distribution curves of tensile strengths for the AU fibers coated by the AZ and ZNP solutions, respectively. Both results show that the strengths of the coated fibers are lower than those of the untreated fibers. This is due to fiber damage occurring in the course of teasing out a single filament from a tow and during subsequent preparation of the fiber for the coating process. However, the strength slightly increases with increasing concentration of the coating solutions, *i.e.*, when a thicker layer of the coating is formed on the fiber. The results of average tensile strengths and Weibull parameters for bimodal distribution of the fibers with different coating conditions at a fixed gage length of 6.5 mm are summarized in Table II. It is to be noted that the scale factors in the Weibull parameters for both low and high strength regions increase as the concentration of the coating solutions increases. From these results, it is evident that the coating blunts the surface cracks which had formed during handling and can also protect the surface against further damage after coating.

Interfacial Shear Strength

The fiber strength, at the critical length, of the untreated AU fiber was estimated by the simulation model using unimodal as well as bimodal Weibull distributions. The average tensile strengths of the fiber tested at the gage lengths of 22, 10, 6.5, and 3 mm are plotted in the Figure 8, and the straight line which is obtained using linear

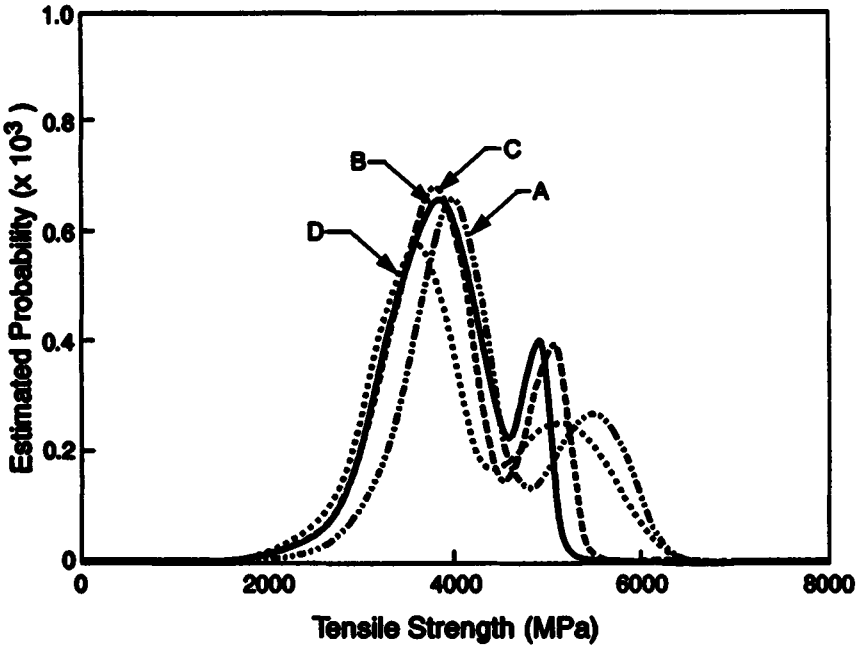

FIGURE 6 Bimodal Weibull distribution of AU fibers coated by AZ solution with different concentrations at gage length of 6.5 mm: a) 0%, b) 1%, c) 3%, d) 5%.

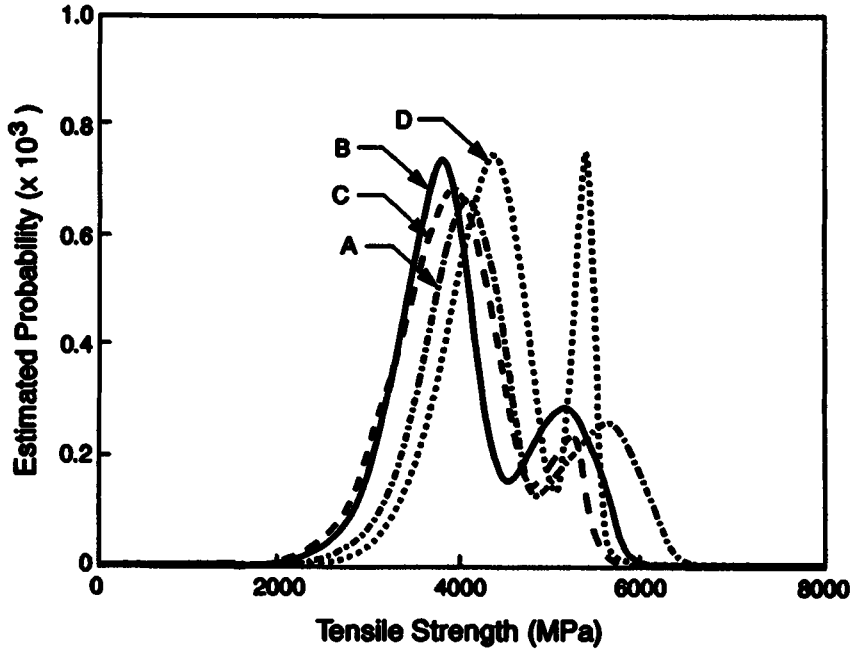

FIGURE 7 Bimodal Weibull distribution of AU fibers coated by ZNP solution with different concentrations at gage length of 6.5 mm: a) 0%, b) 1%, c) 3% and d) 5%.

TABLE II
Average tensile strengths and parameters for bimodal Weibull distributions of AU-type carbon fibers with different coating conditions at gage length of 6.5 mm

Condition	Size	Strength (MPa)	S.D.	p	Weibull m	s_0
untreat	37	4370	838	25/37	10.57	4079
				12/37	12.73	5604
AZ coat.						
1%	52	3900	775	43/52	8.53	3945
				9/52	31.08	4975
3%	43	3980	720	33/43	9.31	3880
				10/43	23.82	5120
5%	40	4110	912	23/40	9.17	3653
				17/40	8.37	5272
ZNP coat.						
1%	44	4000	740	31/44	10.37	3788
				13/44	13.65	5122
3%	35	3900	680	30/35	8.39	3937
				5/35	22.87	5146
5%	38	4400	742	30/38	11.20	4355
				8/38	51.74	5344

p: ratios of low- and high-strength populations.
S. D.: standard deviation.

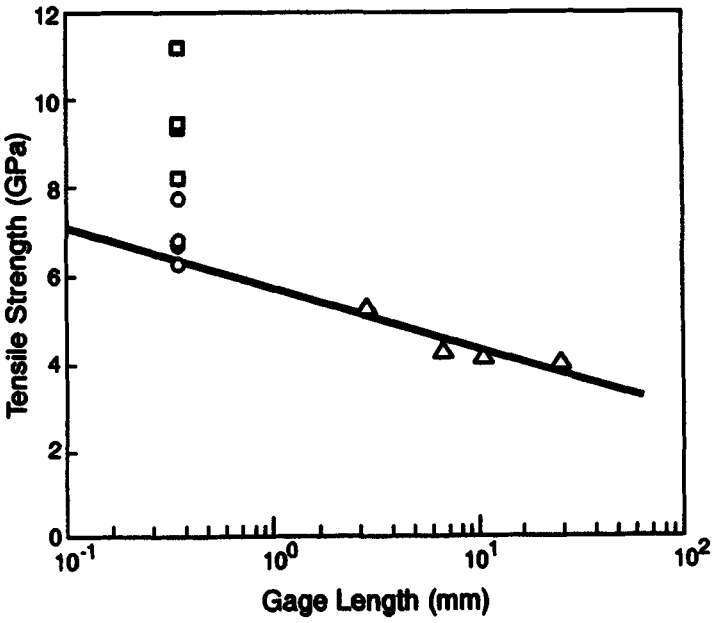

FIGURE 8 Predicted fiber strengths at the critical length (0.36 mm) using unimodal distribution (□) and bimodal distribution (0) of experimental data (△) at gage lengths 22 mm, 10 mm, 6.5 mm and 3 mm for untreated AU fibers.

regression of the strength data with respect to the logarithm of gage length is used to extrapolate to the strength at the critical length. The predicted fiber strengths at the critical length (0.36 mm), obtained by numerical simulation using both bimodal and unimodal distribution with each of the four different gage lengths are also plotted. It is seen that, at the critical length, the strengths estimated by the numerical simulation using bimodal distribution agree with the extrapolated strength using the experimental data, but overestimated strengths are obtained using the unimodal distribution model. It is also found that the strength data obtained using bimodal distribution of strength data at different gage lengths are less scattered than those using unimodal distribution.

Figures 9 and 10 illustrate the average number of fiber breaks plotted as a function of extension of the SFC sample for the fiber coated by the AZ and ZNP solutions, respectively. The number of fiber breaks in the specimen increases continuously with increasing elongation of the specimen. In Figure 9, the average of the maximum number of breaks in AZ-coated fibers in the SFC specimens slightly increases as the concentration of the coating solution increases, but the number of breaks for all coated fibers is less than that for the uncoated fiber. However, the reduction in the maximum number of breaks observed in the SFC specimen of 5% ZNP-coated fibers is much more drastic (Fig. 10). It is inferred that in this case the failure takes place inside the coating rather than at the interface between the fiber. Since the maximum number of fiber breaks for the specimens with fibers coated by

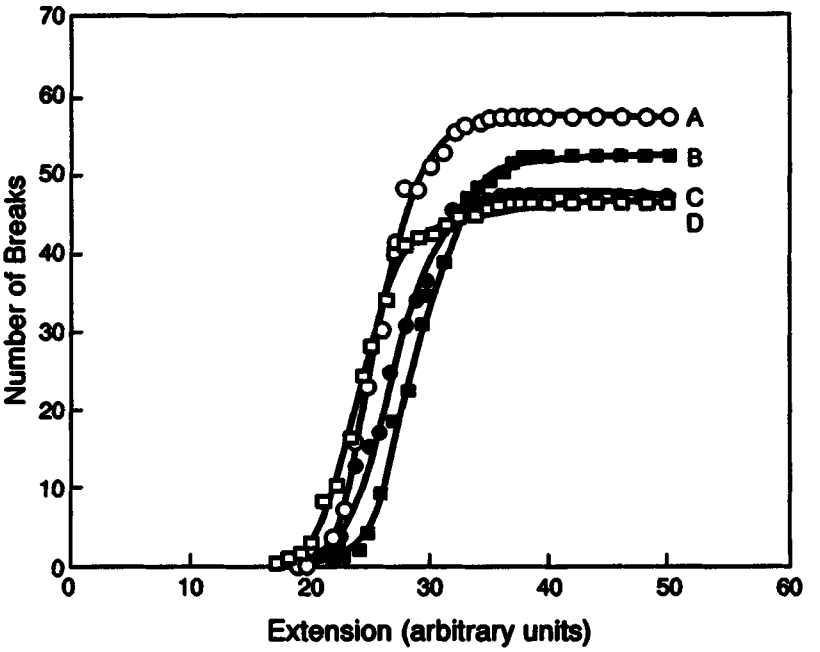

FIGURE 9 Variation of average number of fiber breaks with extension of SFC specimens of AU fiber coated by AZ solutions of different concentrations: a) 0%, b) 1%, c) 3%, d) 5%.

solutions of lower concentration is also less than that for specimens with untreated fiber, it can be inferred that the adhesion of the epoxy resin to the fiber is better than that of the coating to the fiber.

The calculated interfacial shear strengths of the AU fibers coated under different conditions are shown in Table III. The interfacial shear strength (τ_{est}) was calculated by the following equation;

$$\tau_{est} = \frac{\sigma_{sim} \cdot d}{2 \cdot l_c} \tag{9}$$

where σ_{sim} was obtained from numerical simulation using bimodal distribution and l_c was obtained from the SFC test. The calculated results for the interfacial shear strength of the coating to the fiber can be compared to determine the effects of experimental variables. The maximum values of the interfacial shear strength in the case of the coating from the ZNP solution is about 58 MPa and that for the coating from AZ solution is approximately 57 MPa. About 90% of the interfacial shear strength of the uncoated fiber is retained after coating. More detailed experiments are needed in order to make a rigorous evaluation of coatings obtained under carefully controlled conditions. The present results give good support for such investigations on using the coated fibers as reinforcement in a metal matrix.

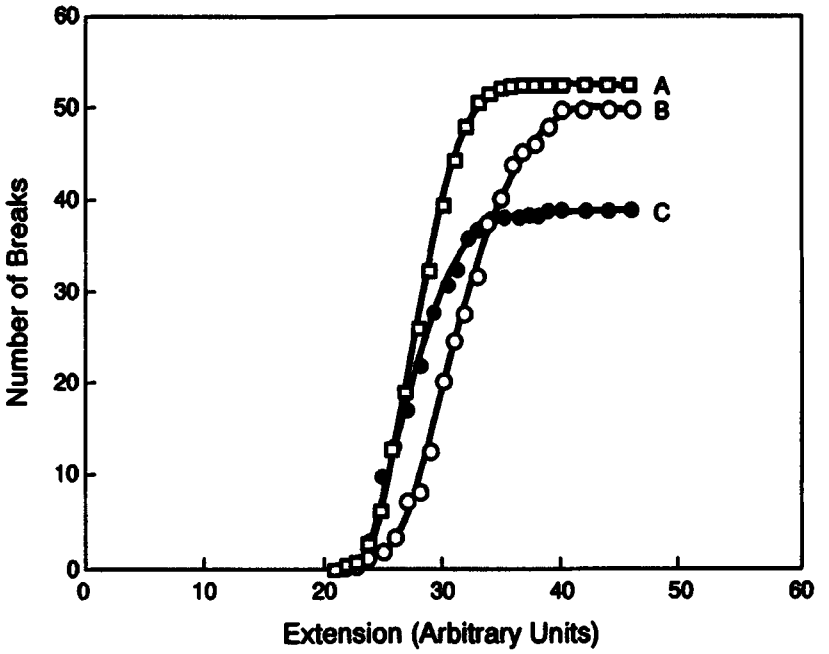

FIGURE 10 Variation of average number of fiber breaks with extension of SFC specimens of AU fiber coated by ZNP solutions of different concentrations: a) 1%, b) 3%, c) 5%.

TABLE III
Interfacial shear strengths of AU-type carbon fibers with different coatings calculated by using predicted maximum strengths of the fibers at the critical length

Condition	$d(\mu m)$	N_{exp}	l_c(mm)	σ_{sim}(MPa)	N_{sim}	τ_{est}(MPa)
untreat.	7.41	59.5	0.3636	6340	64.05	64.6
AZ coat.						
1%	7.48	47.5	0.4536	6220	54.55	51.3
3%	7.49	48.5	0.4444	6130	51.33	51.7
5%	7.49	53.25	0.4055	6210	55.53	57.4
ZNP coat.						
1%	7.52	49.5	0.4356	5800	53.16	50.1
3%	7.45	52.5	0.4112	6450	54.46	58.4
5%	7.55	38.75	0.5535	5610	41.78	38.3

d: diameter of the fiber.
N_{exp}: maximum number of fiber breaks obtained from experiment.
l_c: critical length.
σ_{sim}: fiber strength at the critical length predicted by simulation.
N_{sim}: maximum number of fiber breaks predicted by simulation.
τ_{est}: estimated interfacial shear strength.

CONCLUSIONS

From these results, the following conclusions are obtained. The dip-coating method is applicable to form uniform coatings on the carbon fiber from both the AZ and the ZNP solutions. The weight of the coating is controlled by varying the concentration of coating solutions.

The effects of defects in the fiber are manifested in the gage length dependence of fiber strength and fiber strength distribution. It can be concluded that the untreated AU fiber has at least three kinds of defects. Two of them, one, surface and another, internal, govern fracture of the fiber at gage lengths exceeding 3 mm. At the 3 mm gage length, the third type of defect, probably also internal, controls fiber fracture at the highest strength region. Surface defects characteristic of the lowest strength population, are not operative at this gage length.

The coating process causes some surface damage which results in a slight decrease in the mean fiber strength. However, since the strength increases with increasing concentrations of the coating solutions, and the Weibull scale factors also increase, it is also indicated that the coating blunts the surface cracks formed in handling and also protects against further damage.

The simulation theory used here predicts, with reasonable accuracy, the fiber strength at the critical length, which is impossible to measure experimentally with currently-available methods. Simulation thus eliminates the need for extensive data collection at different gage lengths, which would be required for extrapolation to the critical length. However, it is important to incorporate the experimentally-observed strength distribution in the application of the simulation theory in order to avoid overestimation. The predicted fiber strength at the critical length determined from the SFC test can be used to calculate τ.

The interfacial shear strength is increased slightly as the concentration of the coating solution increases, to reach about 90% of the value for uncoated fibers with the epoxy resin matrix. However, it is also recognized that failure can occur within the coating in thicker coatings. Therefore, it is necessary to arrive at the optimum thickness of coatings in order to avoid undesirable failure such as failure within the coating. The level of bonding achieved between the fiber and the coating is encouraging for potential use of the coated fiber as reinforcement in metal matrix composites, with necessary optimization of the coating process.

References

1. A. Okura and K. Motoki, *Compos. Sci. Technol.* **24**, 243 (1985).
2. J. J. Masson, K. Schulte, F. Girot and Y. LePetitcorps, *Mater. Sci. Eng.* **A135**, 59 (1991).
3. K. K. Chawla, *Composite Materials*, (Springer-Verlag, N. Y., 1987), p. 122.
4. H. Katzmam, *J. Mater. Sci.* **22**, 144 (1987).
5. R. V. Subramanian and E. Nyberg, *J. Mater. Res.* **7**, 677 (1992).
6. A. S. Crasto, S. H. Own and R. V. Subramanian, *Polym. Composites* **9**, 78 (1988).
7. Taehwan Jung, R. V. Subramanian and V. S. Manoranjan, *J. Mater. Sci.* **28**, 4489 (1993).
8. W. A. Curtin, *J. Mater. Sci.* **26**, 5239 (1991).
9. H. Schroeder, *Physics of thin films*, Vol. 5 (Academic Press, N. Y. 1969), p. 87.